Conversion of *Zonulae Occludentes* from Tight to Leaky Strand Type by Introducing Claudin-2 into Madin-Darby Canine Kidney I Cells

Mikio Furuse,* Kyoko Furuse,‡ Hiroyuki Sasaki,‡ and Shoichiro Tsukita*

*Department of Cell Biology, Faculty of Medicine, Kyoto University, Kyoto 606-8501, Japan; and ‡KAN Research Institute Inc., Kyoto 600-8317, Japan

Abstract. There are two strains of MDCK cells, MDCK I and II. MDCK I cells show much higher transepithelial electric resistance (TER) than MDCK II cells, although they bear similar numbers of tight junction (TJ) strands. We examined the expression pattern of claudins, the major components of TJ strands, in these cells: claudin-1 and -4 were expressed both in MDCK I and II cells, whereas the expression of claudin-2 was restricted to MDCK II cells. The dog claudin-2 cDNA was then introduced into MDCK I cells to mimic the claudin expression pattern of MDCK II cells. Interestingly, the TER values of MDCK I clones stably expressing claudin-2 (dCL2-MDCK I) fell to the levels of MDCK II cells (>20-fold decrease). In contrast, when dog claudin-3 was introduced into MDCK I cells, no change was detected in their TER. Similar results were obtained in mouse epithelial cells, Eph4. Morphometric analyses identified no significant differences in the density of TJs or in the number of TJ strands between dCL2-MDCK I and control MDCK I cells. These findings indicated that the addition of claudin-2 markedly decreased the tightness of individual claudin-1/4–based TJ strands, leading to the speculation that the combination and mixing ratios of claudin species determine the barrier properties of individual TJ strands.

Key words: tight junction • *zonula occludens* • claudin • Madin-Darby canine kidney cells • transepithelial electric resistance

Introduction

The *zonula occludens*, or tight junction (TJ),[1] is one mode of cell-to-cell adhesion in vertebrate epithelial and endothelial cellular sheets, and is located at the most apical part of their lateral membranes. On ultrathin section electron microscopy, TJs appear as a zone where plasma membranes of neighboring cells appose very closely, making focal complete contacts (Farquhar and Palade, 1963). On freeze fracture electron microscopy, TJs look like continuous, anastomosing intramembranous particle strands or fibrils (TJ strands) with complementary grooves (Staehelin, 1973, 1974). These observations led to our current understanding of the three-dimensional structure of TJs; each TJ strand associates laterally with another TJ strand in apposing membranes of adjacent cells to form "paired" TJ strands, where the intercellular space is completely obliterated (see Tsukita and Furuse, 2000).

TJs seal the intercellular space between adjacent cells, i.e., create a primary barrier to the diffusion of fluid, electrolytes, and macromolecules through the paracellular pathway (Schneeberger and Lynch, 1992; Gumbiner, 1993; Anderson and van Itallie, 1995). Thus, TJs are essential for epithelial and endothelial cellular sheets to function as diffusion barriers to establish various compositionally distinct fluid compartments in multicellular organisms. Morphological and physiological studies, however, have revealed that TJs are not a simple barrier—they show ion and size selectivity and their barrier function varies significantly in tightness depending on the cell type and physiological requirements. Such regulated and diversified permeability of TJs is thought to be required for dynamically maintaining the interior environment of each compartment (see Powell, 1981; Reuss, 1992; Gumbiner, 1993).

The structural basis for determining and regulating the TJ permeability has been a subject of debate. By comparing the transepithelial electric resistance (TER) and the morphology of TJ strands in various epithelia, Claude and Goodenough (1973) and Claude (1978) found that as TJ strands increase in number, the TER value increases logarithmically. Furthermore, the increase in TER of cultured epithelial cells after plating on permeable filters showed a good correlation with that in the TJ strand number (Madara and Dharmsathaphorn, 1985). This correlation was

Address correspondence to Shoichiro Tsukita, M.D. & Ph.D., Department of Cell Biology, Faculty of Medicine, Kyoto University, Sakyo-ku, Kyoto 606-8501, Japan. Tel.: 81-75-753-4372. Fax: 81-75-753-4660. E-mail: htsukita@mfour.med.kyoto-u.ac.jp

[1]*Abbreviations used in this paper:* E-face, extracellular face; P-face, protoplasmic face; TER, transepithelial electric resistance; TJ, tight junction.

confirmed in various tissues and cells, but exceptions have also been reported (Martinez-Palomo and Erlij, 1975; Mollgard et al., 1976; Frederikson et al., 1979; Martinez-Palomo et al., 1980). One clear exception was found in MDCK epithelial cells, which were originally established from dog kidney (Cereijido et al., 1978). Two strains of MDCK cells, MDCK I and II, have been established that showed functional and biochemical differences including a marked disparity in TER, possibly related to their derivation from different tubules in the kidney (Richardson et al., 1981; Fuller and Simons, 1986; van Meer et al., 1987). Using these two MDCK strains, Stevenson et al. (1988) reported that MDCK I cells showed higher TER than MDCK II cells (>30–60-fold), but that there were no significant differences between these two strains in their morphology or the number of TJ strands. This finding was also confirmed by Gonzalez-Mariscal et al. (1989). These observations conclusively indicated that individual paired TJ strands vary in tightness depending on cell type. However, at that time, mainly due to the lack of information on the molecular architecture of TJ strands themselves, this diversified tightness of individual paired TJ strands was not understood in molecular terms.

Occludin and claudins are now known as constituents of TJ strands (Furuse et al., 1993, 1998a). Both occludin and claudins bear four transmembrane domains, but did not show any sequence similarity with each other. Claudins with molecular masses of ~23 kD comprise a multi-gene family consisting of >20 members (Furuse et al., 1998a; Morita et al., 1999a,b,c; Simon et al., 1999; Tsukita and Furuse, 1999). When each claudin species or occludin was overexpressed in mouse L fibroblasts, claudin molecules, but not occludin, were polymerized within plasma membranes to reconstitute paired TJ strands (Furuse et al., 1998b; Kubota et al., 1999; Morita et al., 1999b,c). Furthermore, when MDCK I cells expressing claudin-1 and -4 were incubated with a claudin-4–binding peptide (the carboxy-terminal half of *Clostridium perfringens* enterotoxin), claudin-4 was specifically removed from TJs, resulting in a significant increase in TJ permeability (Sonoda et al., 1999). These findings indicated that claudins are not only structural but also functional components of TJ strands.

More than two claudin species were shown to be coexpressed in single cells in various tissues (Furuse et al., 1998a, 1999; Morita et al., 1999a). These observations raised the question of how these heterogeneous claudin species are integrated into "paired" TJ strands. Detailed analyses revealed that heterogeneous claudin species are copolymerized to form individual TJ strands as heteropolymers, and that between adjacent TJ strands claudin molecules adhere with each other in both homotypic and heterotypic manners, except in some combinations (Furuse et al., 1999). It is tempting to speculate that variation of the tightness of individual paired TJ strands is determined by the combination and mixing ratios of claudin species (Tsukita and Furuse, 2000). In this study, to evaluate this speculation, we compared two MDCK strains, MDCK I and II, with special attention to claudins, and found that claudin-2 was expressed in MDCK II but not in MDCK I cells. Interestingly, when claudin-2 was introduced into MDCK I cells, their tight TJs were converted to leaky TJs for ions, not for dextran, which were similar not only functionally but also morphologically to those in MDCK II cells. Furthermore, similar conversion of TJ strands was observed when claudin-2 was introduced into mouse epithelial cells, Eph4. These findings favored the suggestion that the combination of claudin species determines the tightness of individual paired TJ strands.

Materials and Methods

Cells and Antibodies

MDCK I cells were obtained from American Tissue Culture Collection and have been maintained in our laboratory. MDCK II cells were provided by Dr. Masayuki Murata (National Institute for Physiological Sciences, Okazaki, Japan). Mouse mammary epithelial cell line, Eph4, was gifted from Dr. Reichman (Institute Suisse de Recherches, Lausanne, Switzerland). Cells were grown in DME supplemented with 10% FCS.

Guinea pig anti–mouse claudin-1 pAb, rabbit anti–mouse claudin-2 pAb, rabbit anti–mouse claudin-3 pAb, and rabbit anti–mouse claudin-4 pAb were raised and characterized as described previously (Furuse et al., 1999; Morita et al., 1999a). Rat anti–occludin mAb (MOC37) and mouse anti–ZO-1 mAb (T8/754) were also described previously (Itoh et al., 1991; Furuse et al., 1993).

Cloning of Dog Claudin-2 and -3 cDNAs, Plasmid Construction, and Transfection

Total RNA was isolated from MDCK II cells according to the method described by Chomczynski and Sacchi (1987), and first strand cDNA was synthesized by reverse transcription using Superscript II™ reverse transcriptase (GIBCO BRL). Using this as a template, the cDNA fragment of dog claudin-2 was amplified by PCR using the sense primer 5′ ATGGCCTCCCTTGGCGTTCAACTGGTGGGC 3′ and the reverse primer 5′ TCACACATACCCAGTCAGGCTGTATGAGTT 3′ that were synthesized according to the nucleotide sequence of mouse claudin-2 (Furuse et al., 1998a). A 700-bp DNA fragment amplified by PCR was cloned into the pGEM-T Easy vector (Promega), and sequencing confirmed that this DNA fragment encoded the dog homologue of claudin-2. The λgt11 dog liver cDNA library (CLONTECH Laboratories, Inc.) was then screened using the 700-bp cDNA fragment as a probe, and one clone, 2-21, containing the whole open reading frame of dog claudin-2 was cloned into pBluescript SK(−) followed by sequencing. This dog claudin-2 cDNA was subcloned into pCAGGSneodelEcoRI (Niwa et al., 1991) to construct the expression vector pCdCL-2. The cDNA encoding dog claudin-3 was isolated and subcloned into the expression vector (pCdCL-3) by the similar procedure.

To obtain MDCK I transfectants expressing dog claudin-2 or -3, MDCK I cells cultured in 35-mm dishes were transfected with a mixture of 1 μg of pCdCL-2 or -3 (or an empty vector, pCAGGSneodelEcoRI, for control) in serum-free DMEM containing 50 μM $CaCl_2$ using LipofectAmine Plus (GIBCO BRL). After an ~10–12-d selection in growth media containing 300 μg/ml of G418, resistant colonies were picked up and screened by immunofluorescence microscopy with anti–claudin-2 or -3 pAb. To obtain Eph4 cells overexpressing mouse claudin-1 or -2, Eph4 cells were transfected with the expression vector pCCL-1 or pCCL-2 (Furuse et al., 1999), respectively, using the same procedure.

Measurement of Transepithelial Electric Resistance and Paracellular Tracer Flux

Aliquots of 1×10^5 or 4×10^5 cells were plated on Transwell filters 12 or 24 mm in diameter, respectively, and the culture medium was exchanged every day. TER was measured directly in culture media using a Millicell-ERS epithelial voltohmmeter (Millipore). The TER values were calculated by subtracting the background TER of blank filters and by multiplying by the surface area of the filter. The TER values reached the maximum levels by 6 d under these experimental conditions.

For paracellular tracer flux assay, FITC-dextran of 4 or 40 kD (Sigma-Aldrich) was dissolved in P buffer (Balda et al., 1996) at a concentration of 10 mg/ml and dialyzed against the same buffer. The media of apical and basolateral compartment of cells grown on Transwell filter were replaced with 250 μl of P buffer containing FITC-dextran and 700 μl P buffer, respectively, and the cells were incubated at 37°C for 3 h. The amount of

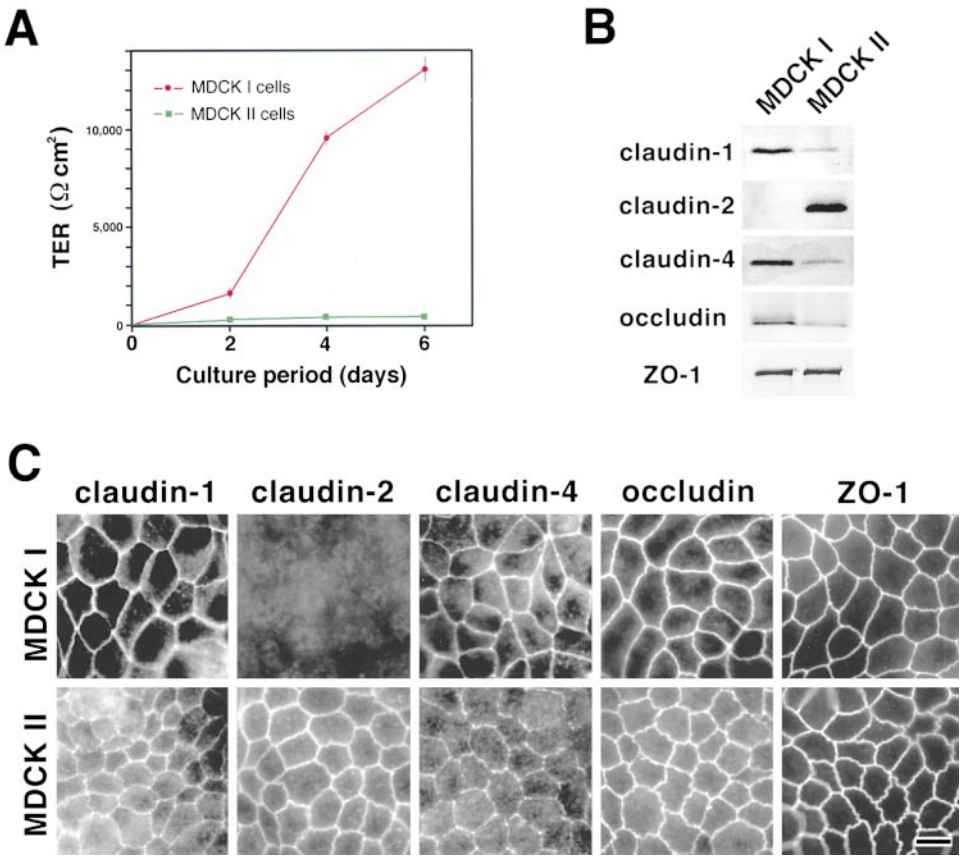

Figure 1. Claudins in MDCK I and II cells. (A) TER measurement of MDCK I and II clones used in this study. MDCK I or II cells (4×10^5 cells) were plated on 24-mm filters. In 6-d culture, the TER values of MDCK I and II cells reached the maximum levels, 12,992 ± 594 and 206 ± 35 Ωcm^2, respectively (mean ± SD, $n = 11$). (B) Immunoblotting. Total lysates of MDCK I and II cells were separated by SDS-PAGE, followed by immunoblotting with pAbs for claudin-1, -2, and -4, and mAbs for occludin and ZO-1. In both MDCK I and II cells, claudin-1 and -4 were expressed, although their expression levels in MDCK II cells were significantly lower than those in MDCK I cells. Claudin-2 was expressed only in MDCK II cells. Occludin was expressed in larger amounts in MDCK I than MDCK II cells. (C) Immunofluorescence microscopy. In MDCK I cells, claudin-1, claudin-4, occludin, and ZO-1 were coconcentrated at TJs, where claudin-2 was undetectable. In contrast, in MDCK II cells, in addition to claudin-1, claudin-4, occludin, and ZO-1, claudin-2 was clearly detected at TJs. The claudin-4 signal was weak. Bar, 10 μm.

FITC-dextran diffused from the apical to the basolateral side of cellular layer was measured by a fluorometer.

SDS-PAGE and Immunoblotting

SDS-PAGE was performed according to the method of Laemmli (1970), and proteins were electrically transferred from gels onto polyvinylene difluoride membranes. The membranes were soaked in 5% skimmed milk and incubated with the primary antibodies. After washing with PBS, the membranes were incubated with biotinylated second antibodies for rabbit, rat, mouse (Amersham Pharmacia Biotech), or guinea pig (Chemicon) IgG. They were then washed with PBS followed by incubation with streptavidin-conjugated alkaline phosphatase (Amersham Pharmacia Biotech). The enzyme reaction was visualized using nitroblue tetrazolium and bromochloroindolyl phosphate. To estimate the amount of claudin-2 in the transfectants, the intensity of the immunoblotted bands were measured by densitometry using Photoshop software.

Immunofluorescence Staining

Immunofluorescence microscopy was performed as described previously (Sonoda et al., 1999). Cells cultured on filters for 6 d were fixed with 10% trichloroacetic acid for 30 min on ice (Hayashi et al., 1999), washed with PBS, and then treated with 0.2% Triton X-100 in PBS for 10 min. After washing with PBS, cells were soaked in 1% BSA in PBS and incubated with primary antibodies for 30 min in a moist chamber. Cells were then washed with PBS and incubated with the fluorescently labeled secondary antibodies for 30 min. FITC-conjugated goat anti–rat IgG (BioSource International), Cy3-conjugated goat anti–rabbit IgG (Amersham Pharmacia Biotech), Cy3-conjugated goat anti–mouse IgG (Amersham Pharmacia Biotech), and rhodamine-conjugated goat anti–guinea pig IgG (Chemicon) were used as secondary antibodies. Cells were washed with PBS and mounted in 90% glycerol-PBS containing 1% paraphenylendiamine and 1% *n*-propylgalate. Specimens were observed using a fluorescence Axiophot photomicroscope (Carl Zeiss, Inc.), and the images were recorded with a Sensys™ cooled CCD camera system (Photometrics).

Linear junctional density (the total length of TJs/area) was determined according to the method described previously (Stevenson et al., 1988). In MDCK cells immunofluorescently stained with anti–ZO-1 mAb, the ZO-1–positive TJs were traced on printed photographs, and the total length of TJs as well as the area were measured using NIH Image 1.62 software.

Freeze-Fracture Electron Microscopy

After cells grown on Transwell filters for 6 d were fixed with 2% glutaraldehyde in 0.1 M sodium cacodylate buffer, pH 7.3, for 24 h at 4°C, they were washed with cacodylate buffer, immersed in 30% glycerol in cacodylate buffer for 2 h, and then frozen in liquid nitrogen. Frozen samples were fractured at −100°C and platinum-shadowed unidirectionally at an angle of 45° in Balzers Freeze Etching System (BAF060; BAL-TEC). Samples were then immersed in household bleach, the replicas floating off the samples were picked up on formovar-filmed grids and examined with a Hitachi H-7500 electron microscope at an acceleration voltage of 100 kV.

The mean strand numbers of TJs were measured on freeze-fracture replica images according to the procedure described by Stevenson et al. (1988). The number of TJ strands was determined by taking numerous counts along a line drawn perpendicular to the junctional axis at 200-nm intervals (Sonoda et al., 1999).

Results

Claudins in MDCK I and II Cells

When MDCK I and II cells were grown on permeable filters for 6 d, confluent monolayers of MDCK I cells

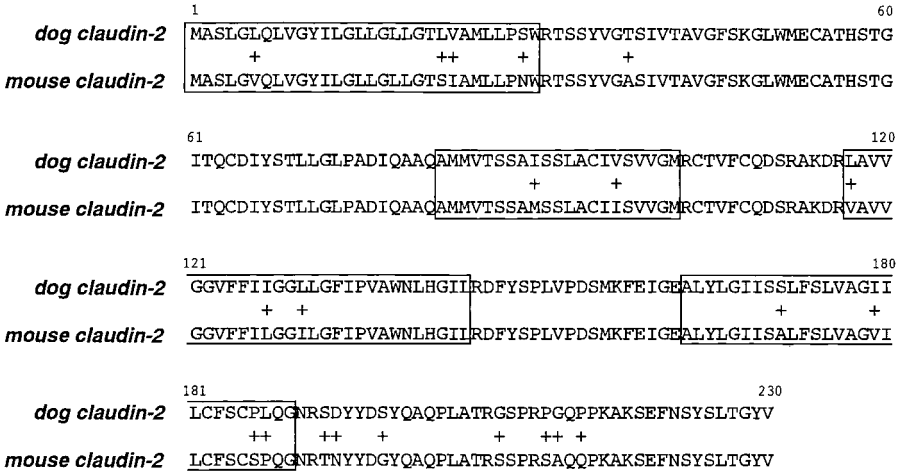

Figure 2. Comparison of amino acid sequences of dog and mouse claudin-2. Nonidentical residues are indicated by +, and four putative transmembrane domains are indicated by boxes. Note that most of the nonidentical residues are distributed within transmembrane domains and the COOH-terminal cytoplasmic domain. The nucleotide sequences of dog claudin-2 and -3 are available at GenBank/EMBL/DDBJ (accession numbers AF358907 and AF358908, respectively).

showed markedly higher TER values than those of MDCK II cells under the culture condition used in this study (Fig. 1 A). Furthermore, by measuring the flux of membrane-impermeable paracellular tracers (FITC-dextran, 40 K), it was confirmed that this TER disparity is not simply due to the disruption of the continuity of TJs (MDCK I, 1,157 ± 379 ng/ml; MDCK II, 3,826 ± 266 ng/ml; mean ± SD, $n = 5$). We then compared the expression of claudins between these two strains by immunoblotting and immunofluorescence microscopy. As reported previously (Sonoda et al., 1999), immunoblotting revealed that MDCK I cells primarily expressed claudin-1 and -4. In contrast, in MDCK II cells claudin-2 was detected abundantly in addition to claudin-1 and -4, the expression levels of which were significantly lower than those in MDCK I cells (Fig. 1 B). No differences were detected in the levels of ZO-1 expression between MDCK I and II cells, but occludin appeared to be expressed in larger amounts in MDCK I than in MDCK II cells.

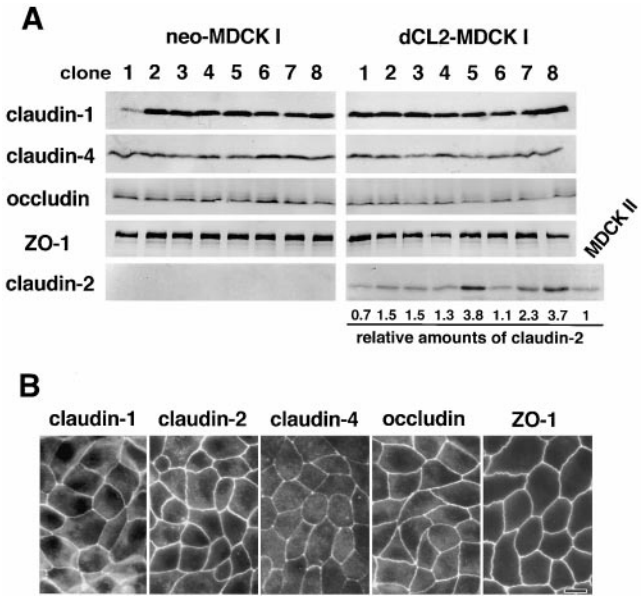

Figure 3. Establishment of MDCK I transfectant clones stably expressing claudin-2. Dog claudin-2 and neomycin-resistance genes were introduced into MDCK I cells, and eight independent clones for each were established (dCL2-MDCK I and neo-MDCK I, respectively). (A) Immunoblotting. Total lysates of neo-MDCK I and dCL2-MDCK I clones (and also MDCK II cells) were subjected to SDS-PAGE in the same amount of total proteins, followed by immunoblotting. There were no significant differences in the expression levels of claudin-1, claudin-4, occludin, or ZO-1, except for the dCL2-MDCK I–specific expression of claudin-2 between neo-MDCK I and dCL2-MDCK I clones. The amounts of endogenous claudin-2 in MDCK II cells as well as exogenous claudin-2 in dCL2-MDCK I cells were quantified as described in Materials and Methods, and their dCL2-MDCK I/MDCK II ratios (relative amounts of claudin-2) were calculated. (B) Immunofluorescence microscopy. In clone 2 of dCL2-MDCK I cells, together with endogenous claudin-1, claudin-4, occludin, and ZO-1, exogenously expressed claudin-2 was coconcentrated at TJs. Bar, 10 μm.

Immunofluorescence microscopic observations were consistent with those of immunoblotting analyses (Fig. 1 C). In MDCK I cells, claudin-1 and -4 were clearly concentrated at TJs, where claudin-2 was not detected. Also, in MDCK II cells, claudin-1 and -4 were detected at TJs, although their signal, especially that of claudin-4, was significantly weaker than that in MDCK I cells. MDCK II cells were characterized by intense claudin-2 signals at TJs. Occludin and ZO-1 were clearly concentrated at TJs in both MDCK I and II cells. Of course, at this stage it was difficult to examine the expression and subcellular distribution of all members of the claudin family in these MDCK cells, but as far as examined using available antibodies, the most characteristic difference between MDCK I and II cells was the MDCK II–specific expression of claudin-2.

Barrier Function of MDCK I Transfectants Expressing Exogenous Claudin-2

The question has naturally arisen of whether the MDCK I transfectants expressing exogenous claudin-2 can mimic MDCK II cells in terms of the barrier property of TJs. If we used mouse claudin-2 cDNA in this transfection experiment, it would be possible that it exhibits some dominant-negative effect in dog epithelial cells such as MDCK cells due to its sequence diversity between mouse and dog. We then cloned dog claudin-2 cDNA using mouse cDNA as a probe. Sequencing identified some substitutions of amino acid residues between mouse and dog claudin-2 (Fig. 2).

Table I. Paracellular Tracer Flux

		neo-MDCK I*		dCL2-MDCK I*	
		mean ± SD	*n*	*mean ± SD*	*n*
FITC-dextran 4 K‡	ng/ml	1683 ± 973	8	1402 ± 523	8 (NS)
FITC-dextran 40 K‡	ng/ml	348 ± 163	8	213 ± 64	8 (NS)
TER	Ωcm^2	11448 ± 1934	8	284 ± 93	8

*Cells (4×10^5 cells) were plated on 24-mm filters and cultured for 6 d before measurements.
‡FITC-dextran (4 or 40 kD; 10 mg/ml) was added to the apical compartment. After a 3-h incubation, the amount of FITC-dextran in the basal compartment media was measured with fluorometer. NS, no significant difference versus neo-MDCK I.

Then, this dog claudin-2 cDNA was introduced into MDCK I cells. As control experiments, only the neomycin-resistance gene was transfected. Cells were screened by immunofluorescence microscopy as well as immunoblotting, and finally eight independent stable clones were obtained each for control (neo-MDCK I) and claudin-2–expressing MDCK I cells (dCL2-MDCK I) (Fig. 3 A). As compared with neo-MDCK I cells (clone 1–8), in dCL2-MDCK I cells no significant differences were detected by immunoblotting in the expression levels of claudin-1, claudin-4, occludin, or ZO-1, except for the exogenous expression of claudin-2. When the expression levels of claudin-2 in dCL2-MDCK I cells were quantitatively compared with that in MDCK II cells, the ratios of dCL2-MDCK I/MDCKII were distributed from 0.7 to 3.8 (Fig. 3 A). Immunofluorescence microscopy revealed that in these dCL2-MDCK I cells, the exogenously expressed claudin-2 was concentrated at TJs together with endogenous claudin-1 and -4 as well as occludin and ZO-1 (Fig. 3 B), although the degree of concentration of exogenous claudin-2 at TJs varied depending on clones.

The TER values of dCL2-MDCK I cells were compared with those of neo-MDCK I cells. As shown in Fig. 4 A, when neo-MDCK I cells were cultured on permeable membranes for 6 d under the conditions described in Materials and Methods, the TER values increased and reached ~10,000 Ωcm^2. These values fairly varied depending on clones, but were comparable with those of parental MDCK I cells (Fig. 1 A). In contrast, all of the dCL2-MDCK I clones exhibited much lower TER values, 150–500 Ωcm^2 in 6-d cultures (Fig. 4 A), which were comparable with those of MDCK II cells (Fig. 1 A). There were some differences in the TER values among clones, but we could not discuss these differences based on the expression level of exogenous claudin-2 in each clone (Fig. 3 A), partly because the TER values of neo-MDCK I cells also varied significantly among clones (Fig. 4 A), and partly because it was difficult to estimate the amounts of claudin-2 concentrated at TJs. Furthermore, we assessed the flux of membrane-impermeable paracellular tracers (FITC-dextran 4 and 40 K) across neo-MDCK I and dCL2-MDCK I cell monolayers. As shown in Table I, these two monolayers with distinct TER showed no difference in the paracellular flux of either FITC-dextran 4 or 40 K. Taken together, we concluded that the introduction of claudin-2 markedly decreased TER of the MDCK I cell layer without disrupting the continuity of TJs.

Next, we tried to examine the effects of the overexpression of claudin-3 on TER of MDCK I cells: similar to claudin-2, endogenous claudin-3 was undetectable in MDCK I cells by anti–mouse claudin-3 pAb (Sonoda et al., 1999). For this purpose, we cloned dog claudin-3 cDNA using mouse cDNA as a probe, and introduced it into MDCK I cells. As shown in Fig. 4 B, independent stable clones were obtained for claudin-3–expressing MDCK I cells (dCL3-MDCK I cells) as well as for control (neo-MDCK I cells). In dCL3-MDCK I cells, exogenous claudin-3 was concentrated at TJs. In contrast to dCL2-MDCK I cells, all of the dCL3-MDCK I clones exhibited 14,000–17,000 Ωcm^2 in 6-d cultures, which were comparable with those of neo-MDCK I cells.

Finally, we checked whether these peculiar effects of exogenous claudin-2 in MDCK I cells could be observed in another type of epithelial cells. Mouse Eph4 cells were then examined, although they exhibited much lower TER values as compared with MDCK I cells (Fig. 4 C). This cell line primarily expressed claudin-1, -3, and -4, but not claudin-2 (data not shown). Mouse claudin-1 and -2 cDNAs as well as the neomycin-resistance gene were introduced into Eph4 cells, and several independent stable clones were obtained each for claudin-1–overexpressing Eph4 cells (mCL1-Eph4), claudin-2–expressing Eph4 cells (mCL2-Eph4), and control cells (neo-Eph4). Interestingly, as shown in Fig. 4 C, mCL1-Eph4 cells and neo-Eph4 cells showed similar TER values, 2,000–5,000 Ωcm^2 in 6-d cultures, whereas mCL2-Eph4 cells exhibited much lower TER values, 200–600 Ωcm^2. Thus, we concluded that the introduction of claudin-2, but not claudin-1, decreased TER also in the Eph4 cell layer.

Table II. Morphometric Analyses of TJs in dCL2-MDCK I and neoMDCK I Cells

	Linear junctional density*	Mean number of strands‡	TER§	Cell density‖
	mm/mm²		*Ωcm²*	*n/mm²*
dCL2-MDCK I¶				
clone 2	168 (0.107)	5.1 ± 1.7 (255) NS	514 ± 46	5,181 ± 557
clone 4	183 (0.098)	4.8 ± 1.8 (206) NS	380 ± 43	5,786 ± 678
neo-MDCK I¶				
clone 7	180 (0.113)	4.2 ± 1.6 (210)	13,360 ± 202	5,847 ± 545
clone 8	175 (0.098)	4.7 ± 1.8 (494)	12,998 ± 552	4,734 ± 367

*Total length of TJs (ZO-1–positive lines in focus) per area. Measured area (mm^2) is represented in parentheses.
‡Number of TJ strands along a line drawn perpendicular to the junctional axis. Number of fields examined is represented in parentheses. NS, no significant difference versus clones 7 and 8.
§12 filters were measured for each.
‖Cell density was measured in 20 fields for each.
¶Cells (4×10^5 cells) were plated on 24-mm filters and cultured for 6 d before measurements.

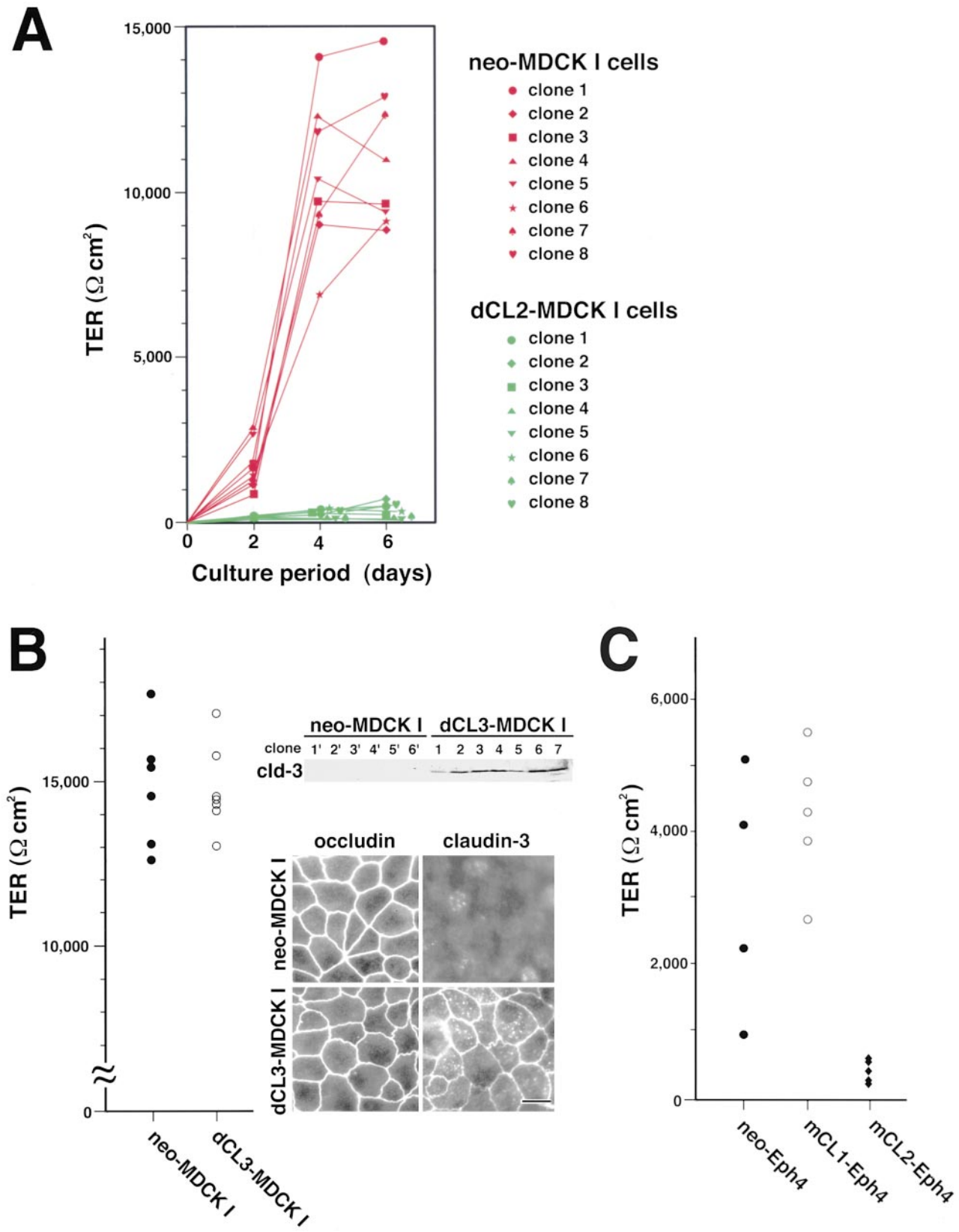

Figure 4. TER measurements of cultured epithelial cells. (A) Barrier properties of dCL2-MDCK I cells. Control neo-MDCK I cells (clone 1–8) and dCL2-MDCK I cells (clone 1–8) (10^5 cells) were plated on 12-mm filters. In 6-d culture, all clones of neo-MDCK I cells exhibited fairly high TER values (Ωcm^2) (mean ± SD, $n = 6$ for each clone) (clone 1, 14,465 ± 1,028; clone 2, 8,753 ± 444; clone 3, 9,686 ± 1,545; clone 4, 10,978 ± 822; clone 5, 9,358 ± 198; clone 6, 9,034 ± 1,588; clone 7, 12,140 ± 318; clone 8, 12,888 ± 376). In contrast, in all clones of dCL2-MDCK I cells, the TER values fell to 150 ~ 500 Ωcm^2 (mean ± SD, $n = 6$ for

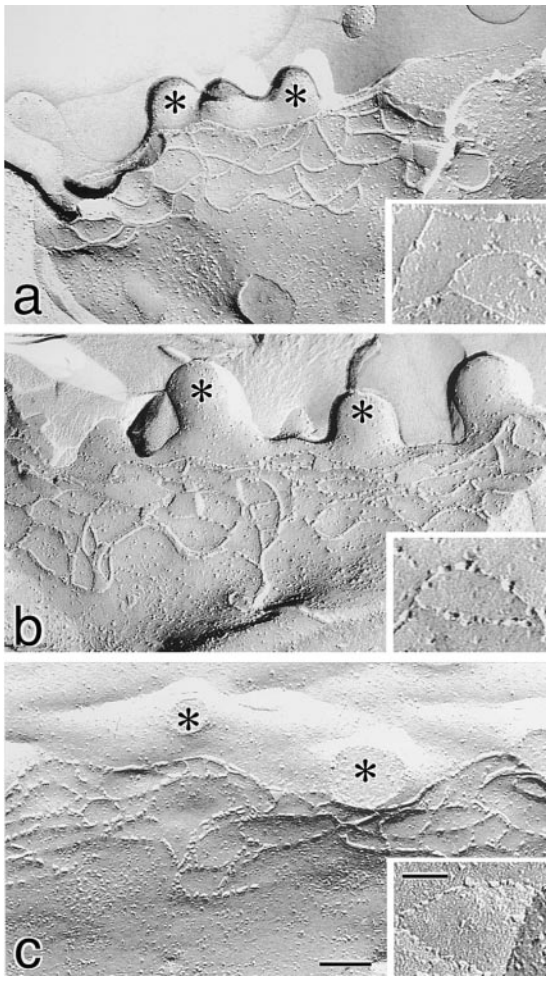

Figure 5. Freeze-fracture replica images of TJs in neo-MDCK I (a), dCL2-MDCK I (b), and MDCK II cells (c). Cells (4×10^5 cells) were plated on 24-mm filters, cultured for 6 d, fixed with glutaraldehyde, and then processed for freeze-fracture replica electron microscopy. The number of TJ strands in neo-MDCK I cells was similar to those in dCL2-MDCK I as well as MDCK II cells (Table II), and the network pattern of TJ strands in neo-MDCK I cells did not appear to be more complex than that in dCL2-MDCK I or MDCK II cells. In neo-MDCK I cells (a), TJ strands were largely associated with the P-face and were mostly continuous, and on the E-face (inset) complementary continuous grooves were vacant. In dCL2-MDCK I cells (b), TJ strands were fairly discontinuous on the P-face, and on the E-face (inset) intramembranous particles were scattered within the grooves. The strands (c) and grooves (inset) of MDCK II cells were similar in appearance to those in dCL2-MDCK I cells. *Microvilli. Bar, 100 nm; inset, 50 nm.

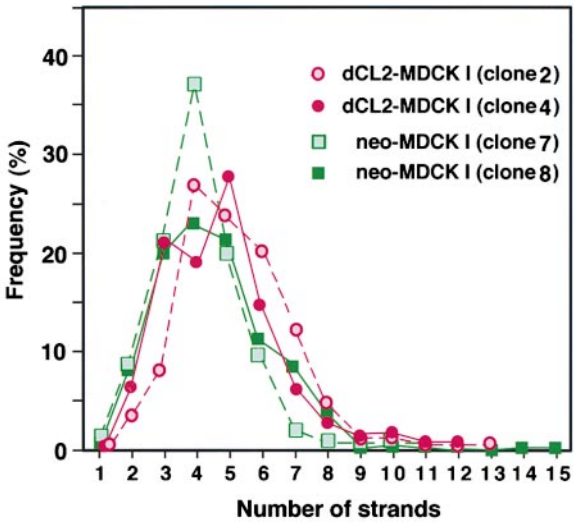

Figure 6. Distribution of the frequency of observation of a given number of TJ strands in dCL2-MDCK I (clones 2 and 4) and neo-MDCK I cells (clones 7 and 8). Using printed pictures of freeze-fracture replica images (Fig. 5), we took numerous counts along a line drawn perpendicular to the junctional axis at 200-nm intervals (Sonoda et al., 1999). From these distribution curves, the mean TJ strand number was determined for each clone (Table II).

Morphology of Tight Junctions in MDCK I Transfectants Expressing Exogenous Claudin-2

The morphology of TJs in dCL2-MDCK I cells was then examined at the light as well as electron microscopic levels. First, two clones of dCL2-MDCK I cells (clones 2 and 4; Fig. 4 A) and neo-MDCK I cells (clones 7 and 8; Fig. 4 A) were immunofluorescently stained with anti–ZO-1 mAb, and the linear junctional density (mm/mm^2; the length of TJs/area) was determined in these clones by tracing the ZO-1–positive lines. As shown in Table II, no differences were detected in the linear junctional density between dCL2-MDCK I and neo-MDCK I clones.

Then, we examined TJs of the above clones of dCL2-MDCK I and neo-MDCK I cells by freeze–fracture electron microscopy. As shown in Fig. 5, the network pattern of TJ strands of dCL2-MDCK I clones was very similar to that of neo-MDCK I clones. To compare these networks quantitatively, the mean number of TJ strands in each clone was determined by making numerous counts of TJ strands along a line drawn perpendicular to the junctional axis according to the method described previously (Stevenson et al., 1988). As summarized in Fig. 6 and Table II, although the mean number of TJ strands varied to some extent, there was no tendency for the number of strands in

each clone) (clone 1, 478 ± 32; clone 2, 510 ± 27; clone 3, 285 ± 14; clone 4, 228 ± 9; clone 5, 188 ± 32; clone 6, 244 ± 18; clone 7, 161 ± 13; clone 8, 316 ± 14). (B) Barrier properties of dCL3-MDCK I cells. Immunoblotting and immunofluorescence microscopy with anti–claudin-3 pAb confirmed the expression of exogenous claudin-3 as well as its concentration at TJs in dCL3-MDCK I cells (right). Control neo-MDCK I cells (six clones) and dCL3-MDCK I cells (seven clones) (10^5 cells) were plated on 12-mm filters. In 6-d culture, both neo- and dCL3-MDCK I cells exhibited fairly high TER values, 14,000–17,000 Ωcm^2 (left). (C) Barrier properties of mCL1- and mCL2-Eph4 cells. Control neo-Eph4 cells (four clones), mCL1-Eph4 cells (five clones), and mCL2-Eph4 cells (five clones) (10^5 cells) were plated on 12-mm filters. In 6-d culture, both neo-Eph4 cells and mCL1-Eph4 cells showed similar TER values, 2,000–5,000 Ωcm^2, whereas mCL2-Eph4 cells exhibited much lower TER values, 200–600 Ωcm^2.

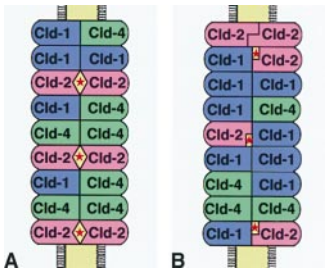

Figure 7. Two models of paired TJ strands consisting of claudin-1, -2, and -4. (A) Homotypic adhesion of claudin-2 within paired strands constitutes aqueous pores with high conductance (*). (B) Heterotypic adhesion between claudin-1 and -2 constitutes aqueous pores with high conductance (*). See text for details.

dCL2-MDCK I clones to be less than that of neo-MDCK I clones.

Although no significant differences were detected in the network pattern of TJs per se, the appearance of individual TJ strands appeared to differ between dCL2-MDCK I and neo-MDCK I clones. As reported previously in MDCK I cells, neo-MDCK I cells showed the typical "protoplasmic (P-) face–associated" TJs; TJ strands were largely associated with the P-face and were mostly continuous, and on the extracellular (E-) face complementary continuous vacant grooves were identified (Fig. 5 a). In contrast, significant numbers of TJ strand particles were associated with the E-face in dCL2-MDCK I cells; TJ strands were fairly discontinuous on the P-face, and on the E-face intramembranous particles were scattered within the grooves (Fig. 5 b). Interestingly, the appearance of TJ strands in dCL2-MDCK I cells was similar to that in MDCK II cells (Fig. 5 c).

Discussion

As discussed by Stevenson et al. (1988), two strains of MDCK cells, MDCK I and II, which bear tight and leaky TJs, respectively, provide a good system in which to examine the molecular basis for the diversity of tightness of individual TJ strands. Now that claudins have been identified as structural as well as functional components of TJ strands (Furuse et al., 1998a,b; Gow et al., 1999; Sonoda et al., 1999; Tsukita and Furuse, 1999, 2000), in this study we compared MDCK I and II strains from the viewpoint of claudins. MDCK I cells expressed primarily claudin-1 and -4, whereas MDCK II cells expressed large amounts of claudin-2 in addition to claudin-1 and -4. We then introduced dog claudin-2 cDNA into MDCK I cells to obtain stable transfectants (dCL2-MDCK I cells). Interestingly, dCL2-MDCK I cells exhibited lower TER values than control MDCK I cells (neo-MDCK I cells). Similar effects of claudin-2 on the TER were observed in mouse epithelial cells, Eph4. Morphometric analyses at both the light and electron microscopic levels revealed that there were no significant differences in the mean number of TJ strands between dCL2-MDCK I and neo-MDCK I cells (Table II and Fig. 6). Furthermore, dCL2- and neo-MDCK I cells showed no difference in the paracellular flux of dextran, confirming the continuity of TJs in dCL2-MDCK I cells. We thus concluded that the individual TJ strands in dCL2-MDCK I cells are leakier for ions than those in neo-MDCK I cells, and that incorporation of claudin-2 into the claudin-1/4–based TJ strands converted the "tight" strands to the "leaky" strands. Furthermore, taking the previous results of Stevenson et al. (1988) into consideration, dCL2-MDCK I cells were indistinguishable from MDCK II cells in terms of their expression pattern of claudins, the expression level of claudin-2 (Fig. 3 A), network pattern and number of TJ strands, and TER values. Therefore, it is tempting to speculate that the difference in the TER value between MDCK I and II cells can be explained by the expression of claudin-2.

Recently, in the freeze-fracture replica images of glutaraldehyde-fixed samples, the extent of association of TJ strand particles to the P-face was demonstrated to be correlated well with the tightness of individual TJ strands in epithelial as well as endothelial cells; i.e., tight and leaky TJs show P- and E-face association of particles, respectively (Wolburg et al., 1994). Cultured brain endothelial cells bear the E-face–associated type of TJs and show loose TJ barrier function but, when these cells are treated with astrocyte-conditioned medium to elevate their intracellular cAMP level, the transendothelial electric resistance increases markedly with concomitant switching of TJs from the E- to the P-face–associated type. Interestingly, in this study, we showed that the introduction of claudin-2 into MDCK I cells shifted the freeze-fracture morphology of TJs from the P-face–associated toward the E-face–associated type. In good agreement, the TJs in MDCK II cells were reported to be somehow E-face–associated (see Wolburg et al., 1994). Although the molecular mechanism behind the P- as well as E-face association in fixed samples remains unknown, these observations were highly consistent with the notion that the individual TJ strands in MDCK I cells were tighter than those in dCL2-MDCK I cells as well as MDCK II cells.

Detailed electrophysiological analyses suggested the existence of aqueous pores within the paired TJ strands (Diamond, 1977; Claude, 1978; Reuss, 1992; Gumbiner, 1993). Stevenson et al. (1988) then discussed the possibility that MDCK I and II cells have very different channel characteristics caused by differences in the probability of the hypothetical aqueous pores in TJ strands being open and closed. Therefore, it is reasonable to speculate that claudin-2 is involved in the formation of aqueous pores with high conductance within the paired TJ strands in MDCK II cells. It is possible that claudin-2 forms such pores through its homotypic adhesion within paired claudin-1/4–based TJ strands (Fig. 7 A). However, as we discussed previously (Tsukita and Furuse, 2000), it is also possible that the weak heterotypic adhesion of claudin-2 with claudin-1 (or -4) results in the formation of aqueous pores with high conductance within the paired TJ strands (Fig. 7 B). Claudin-2 does not adhere strongly with claudin-1 in a heterotypic manner in L fibroblast transfectants (Furuse et al., 1999), but a homopolymer of claudin-1 makes a paired strand with a heteropolymer consisting of claudin-1 and -2 in L fibroblast transfectants (our unpublished data; see Tsukita and Furuse, 2000). Therefore, aqueous pores with a high probability of being in the open state would be formed between claudin-1 and -2 when they are apposed within paired TJ strands (Fig. 7 B). In this connection, it is interesting to point out that the overexpression of claudin-3 into MDCK I cells as well as that of claudin-1 into Eph4 cells did not affect the barrier functions of TJs (Fig. 4, B and C). As claudin-1 can adhere with claudin-3 (and prob-

ably with claudin-4) in a heterotypic manner (Furuse et al., 1999), aqueous pores with high conductance would not be formed in claudin-1– or -3–overexpressed TJ strands. Furthermore, these findings excluded the possibility that the introduction of claudin-2 affected the TJ barrier function due to the unbalance between the total amounts of claudins and other TJ components such as ZO-1 (McCarthy et al., 2000).

The present results revealed experimentally that the combination and mixing ratios of claudin species determine the tightness of individual TJ strands. However, it is also likely that under some conditions individual TJ strands vary in tightness without changing their claudin combination: transfection experiments with mutant occludin into MDCK cells suggested that occludin is also involved in the determination of tightness of individual strands (Balda et al., 1996, 2000; Bamforth et al., 1999). Treatment with an actin-depolymerizing agent as well as ATP depletion also decreased TER values of epithelial cells (Bacallao et al., 1994; Takakuwa et al., 2000).

The tightness of TJs has been suggested to be determined not only by the tightness of individual TJ strands but also by the number of TJ strands (the mean strand number) (Claude and Goodenough, 1973; Claude, 1978; Madara and Dharmsathaphorn, 1985). For example, in the kidney, epithelial cells of the proximal and distal tubules bear one to two and four to seven TJ strands, respectively, and the epithelial cells of the distal tubules exhibit much higher TER than those of proximal tubules (Claude and Goodenough, 1973). The molecular mechanism behind the determination of the number of TJ strands, however, remains elusive. As we reported previously, when claudin-4 was specifically removed from TJs in MDCK I cells, the mean strand number decreased significantly with concomitant downregulation of their barrier function (Sonoda et al., 1999). In contrast, in the present study, although claudin-2 was overexpressed in MDCK I cells, there was no significant increase in the mean strand number in these transfectants (Fig. 6). McCarthy et al. (2000) also reported that overexpression of wild-type claudin-1 in MDCK cells did not result in the formation of aberrant TJ strands. Therefore, the number of TJ strands appears not to be determined simply by the total amounts of claudins expressed in individual cells.

There are various physiological requirements for paracellular permeability depending on the types of tissues. As discussed above, the degree of paracellular permeability appeared to be determined by multiple factors. Previous analyses of MDCK I and II cells by Stevenson et al. (1988) showed that the tightness of individual TJ strands is variable, and that it is an important factor to determine the paracellular permeability. This study revealed that incorporation of claudin-2 converts the tight TJ strands to leaky strands in MDCK I cells. We then concluded that the combination and mixing ratios of claudin species are important factors to determine the tightness of individual TJ strands. Therefore, it is tempting to speculate that the occurrence of the large number of claudin species allows various organs to exhibit their own appropriate TJ permeability. On the other hand, under pathological conditions, the tightness of individual TJ strands may be changed when expression of one of the claudin species constituting TJ strands is down- or upregulated. It was recently reported that in the thick ascending limb of Henle of patients suffering from hereditary hypomagnesemia, one specific claudin species, paracellin-1/claudin-16, is affected, resulting in a marked decrease in the permeability of TJs for Mg^{2+} as well as Ca^{2+} ions (Simon et al., 1999). Various pathological states and diseases caused by alterations in the tightness of individual TJ strands will probably be identified in the future studies.

We thank all the members of our laboratory for helpful discussions. Our thanks are also due to Ms. K. Yoshida and Ms. K. Hirao-Minakuchi for their excellent technical assistance.

This study was supported in part by a Grant-in-Aid for Cancer Research and a Grant-in-Aid for Scientific Research (A) from the Ministry of Education, Science and Culture of Japan to S. Tsukita, and by the Japan Society for the Promotion of Science Research for the Future Program to M. Furuse.

Submitted: 16 October 2000
Revised: 1 March 2001
Accepted: 1 March 2001

References

Anderson, J.M., and C.M. van Itallie. 1995. Tight junctions and the molecular basis for regulation of paracellular permeability. *Am. J. Physiol.* 269:G467–G475.

Bacallao, R., A. Garfinkel, S. Monke, G. Zampighi, and L.J. Mandel. 1994. ATP depletion: a novel method to study junctional properties in epithelial tissues. I. Rearrangement of the actin cytoskeleton. *J. Cell Sci.* 107:3301–3313.

Balda, M.S., C. Flores-Maldonado, M. Cereijido, and K. Matter. 2000. Multiple domains of occludin are involved in the regulation of paracellular permeability. *J. Cell Biochem.* 78:85–96.

Balda, M.S., J.A. Whitney, C. Flores, S. González, M. Cereijido, and K. Matter. 1996. Functional dissociation of paracellular permeability and transepithelial electrical resistance and disruption of the apical-basolateral intramembrane diffusion barrier by expression of a mutant tight junction membrane protein. *J. Cell Biol.* 134:1031–1049.

Bamforth, S.D., U. Kniesel, H. Wolburg, B. Engelhardt, and W. Risau. 1999. A dominant mutant of occludin disrupts tight junction structure and function. *J. Cell Sci.* 112:1879–1888.

Cereijido, M., E.S. Robbins, W.J. Dolan, C.A. Rotunno, and D.D. Sabatini. 1978. Polarized monolayers formed by epithelial cells on permeable and translucent support. *J. Cell Biol.* 77:853–880.

Chomczynski, P., and N. Sacchi. 1987. Single-step method of RNA isolation by acid guanidinium thiocyanate-phenol-chloroform extraction. *Anal. Biochem.* 162:156–159.

Claude, P. 1978. Morphological factors influencing transepithelial permeability: a model for the resistance of the zonula occludens. *J. Membr. Biol.* 10:219–232.

Claude, P., and D.A. Goodenough. 1973. Fracture faces of zonulae occludentes from "tight" and "leaky" epithelia. *J. Cell Biol.* 58:390–400.

Diamond, J. 1977. The epithelial junction: bridge, gate, and fence. *Physiologist.* 20:10–18.

Farquhar, M.G., and G.E. Palade. 1963. Junctional complexes in various epithelia. *J. Cell Biol.* 17:375–412.

Frederikson, O., K. Mollgard, and J. Rostgaard. 1979. Lack of correlation between transepithelial transport capacity and paracellular pathway ultrastructure in Alcian blue–treated rabbit gall bladders. *J. Cell Biol.* 80:383–393.

Fuller, S.D., and K. Simons. 1986. Transferrin receptor polarity and recycling accuracy in "tight" and "leaky" strains of Madin-Darby canine kidney cells. *J. Cell Biol.* 103:1767–1779.

Furuse, M., K. Fujita, T. Hiiragi, K. Fujimoto, and S. Tsukita. 1998a. Claudin-1 and -2: novel integral membrane proteins localizing at tight junctions with no sequence similarity to occludin. *J. Cell Biol.* 141:1539–1550.

Furuse, M., T. Hirase, M. Itoh, A. Nagafuchi, S. Yonemura, Sa. Tsukita, and Sh. Tsukita. 1993. Occludin: a novel integral membrane protein localizing at tight junctions. *J. Cell Biol.* 123:1777–1788.

Furuse, M., H. Sasaki, K. Fujimoto, and S. Tsukita. 1998b. A single gene product, claudin-1 or -2, reconstitutes tight junction strands and recruits occludin in fibroblasts. *J. Cell Biol.* 143:391–401.

Furuse, M., H. Sasaki, and S. Tsukita. 1999. Manner of interaction of heterogeneous claudin species within and between tight junction strands. *J. Cell Biol.* 147:891–903.

Gonzalez-Mariscal, L., B. Chaves de Ramirez, A. Lazaro, and M. Cereijido. 1989. Establishment of tight junctions between cells from different animal species and different sealing capacities. *J. Membr. Biol.* 107:43–56.

Gow, A., C.M. Southwood, J.S. Li, M. Pariali, G.P. Riordan, S.E. Brodie, J. Da-

nias, J.M. Bronstein, B. Kachar, and R.A. Lazzarini. 1999. CNS myelin and Sertoli cell tight junction strands are absent in OSP/claudin-11 null mice. *Cell.* 99:649–659.

Gumbiner, B. 1993. Breaking through the tight junction barrier. *J. Cell Biol.* 123:1631–1633.

Hayashi, K., S. Yonemura, T. Matsui, Sa. Tsukita, and Sh. Tsukita. 1999. Immunofluorescence detection of ezrin/radixin/moesin (ERM) proteins with their carboxyl-terminal threonine phosphorylated in cultured cells and tissues: application of a novel fixation protocol using trichloroacetic acids (TCA) as a fixative. *J. Cell Sci.* 112:1149–1158.

Itoh, M., S. Yonemura, A. Nagafuchi, Sa. Tsukita, and Sh. Tsukita. 1991. A 220-kD undercoat-constitutive protein: its specific localization at cadherin-based cell-cell adhesion sites. *J. Cell Biol.* 115:1449–1462.

Kubota, K., M. Furuse, H. Sasaki, N. Sonoda, K. Fujita, A. Nagafuchi, and S. Tsukita. 1999. Ca^{++}-independent cell adhesion activity of claudins, integral membrane proteins of tight junctions. *Curr. Biol.* 9:1035–1038.

Laemmli, U.K. 1970. Cleavage of structural proteins during the assembly of the head of bacteriophage T4. *Nature.* 227:680–685.

McCarthy, K.M., S.A. Francis, J.M. McCormack, J. Lai, R.A. Rogers, I.B. Skare, R.D. Lynch, and E.E. Schneeberger. 2000. Inducible expression of claudin-1-myc but not occludin-VSV-G results in aberrant tight junction strand formation in MDCK cells. *J. Cell Sci.* 113:3387–3398.

Madara, J.L., and K. Dharmsathaphorn. 1985. Occluding junction structure–function relationships in a cultured epithelial monolayer. *J. Cell Biol.* 101: 2124–2133.

Martinez-Palomo, A., and D. Erlij. 1975. Structure of tight junctions in epithelia with different permeability. *Proc. Natl. Acad. Sci. USA.* 72:4487–4491.

Martinez-Palomo, A., I. Meza, G. Beaty, and M. Cereijido. 1980. Experimental modulation of occluding junctions in a cultured transporting epithelium. *J. Cell Biol.* 87:736–745.

Mollgard, K., D.N. Malinowski, and N.R. Saunders. 1976. Lack of correlation between tight junction morphology and permeability properties in developing choroid plexus. *Nature.* 264:293–294.

Morita, K., M. Furuse, K. Fujimoto, and S. Tsukita. 1999a. Claudin multigene family encoding four-transmembrane domain protein components of tight junction strands. *Proc. Natl. Acad. Sci. USA.* 96:511–516.

Morita, K., H. Sasaki, K. Fujimoto, M. Furuse, and S. Tsukita. 1999b. Claudin-11/OSP-based tight junctions in myelinated sheaths of oligodendrocytes and Sertoli cells in testis. *J. Cell Biol.* 145:579–588.

Morita, K., H. Sasaki, M. Furuse, and S. Tsukita. 1999c. Endothelial claudin: claudin-5/TMVCF constitutes tight junction strands in endothelial cells. *J. Cell Biol.* 147:185–194.

Niwa, H., K. Yamamura, and J. Miyazaki. 1991. Efficient selection for high-expression transfectants with a novel eukaryotic vector. *Gene.* 108:193–200.

Powell, D.W. 1981. Barrier function of epithelia. *Am. J. Physiol.* 241:G275–G288.

Reuss, L. 1992. Tight junction permeability to ions and water. *In* Tight Junctions. M. Cereijido, editor. CRC Press, London, UK. 49–66.

Richardson, J.C.W., V. Scalera, and N.L. Simmons. 1981. Identification of two strains of MDCK cells which resemble separate nephron tubule segments. *Biochim. Biophys. Acta.* 673:26–36.

Schneeberger, E.E., and R.D. Lynch. 1992. Structure, function, and regulation of cellular tight junctions. *Am. J. Physiol.* 262:L647–L661.

Simon, D.B., Y. Lu, K.A. Choate, H. Velazquez, E. Al-Sabban, M. Praga, G. Casari, A. Bettinelli, G. Colussi, J. Rodriguez-Soriano, et al. 1999. Paracellin-1, a renal tight junction protein required for paracellular Mg^{2+} resorption. *Science.* 285:103–106.

Sonoda, N., M. Furuse, H. Sasaki, S. Yonemura, J. Katahira, Y. Horiguchi, and S. Tsukita. 1999. *Clostridium perfringens* enterotoxin fragment removes specific claudins from tight junction strands: evidence for direct involvement of claudins in tight junction barrier. *J. Cell Biol.* 147:195–204.

Staehelin, L.A. 1973. Further observations on the fine structure of freeze-cleaved tight junctions. *J. Cell Sci.* 13:763–786.

Staehelin, L.A. 1974. Structure and function of intercellular junctions. *Int. Rev. Cytol.* 39:191–283.

Stevenson, B.R., J.M. Anderson, D.A. Goodenough, and M.S. Mooseker. 1988. Tight junction structure and ZO-1 content are identical in two strains of Madin-Darby canine kidney cells which differ in transepithelial resistance. *J. Cell Biol.* 107:2401–2408.

Takakuwa, R., Y. Kokai, T. Kojima, T. Akatsuka, H. Tobioka, N. Sawada, and M. Mori. 2000. Uncoupling of gate and fence functions of MDCK cells by the actin-depolymerizing reagent mycalolide B. *Exp. Cell Res.* 257:238–244.

Tsukita, S., and M. Furuse. 1999. Occludin and claudins in tight junction strands: leading or supporting players? *Trends Cell Biol.* 9:268–273.

Tsukita, S., and M. Furuse. 2000. Pores tin the wall: claudins constitute tight junction strands containing aqueous pores. *J. Cell Biol.* 149:13–16.

van Meer, G., E.H.K. Stelzer, R.W. Wijnaendts-van-Resandt, and K. Simons. 1987. Sorting of sphingolipids in epithelial (Madin-Darby canine kidney) cells. *J. Cell Biol.* 105:1623–1635.

Wolburg, H., J. Neuhaus, U. Kniesel, B. Krauss, E.M. Schmid, M. Öcalan, C. Farrell, and W. Risau. 1994. Modulation of tight junction structure in blood–brain barrier endothelial cells. Effects of tissue culture, second messengers and cocultured astrocytes. *J. Cell Sci.* 107:1347–1357.